3-D Analytic Signal in the Interpretation of Total Magnetic Field Data at Low Magnetic Latitudes

Article *in* Exploration Geophysics · September 1993

DOI: 10.1071/EG993679

3 authors, including:

Ian Macleod
Geosoft Inc.
16 PUBLICATIONS **638** CITATIONS

SEE PROFILE

Exploration Geophysics (1993) **24**, 679–688

3-D Analytic Signal in the Interpretation of Total Magnetic Field Data at Low Magnetic Latitudes

Ian N. MacLeod
Geosoft Inc.
Suite 500
204 Richmond Street West
Toronto, Ontario
M5V 1V6
Canada

Keith Jones
Ashton Mining Limited
24 Outram Street
West Perth, WA 6005
PO Box 962
West Perth, WA 6872

Ting Fan Dai
Geosoft Inc.
Suite 500
204 Richmond Street West
Toronto, Ontario
M5V 1V6
Canada

Abstract

The interpretation of magnetic field data at low magnetic latitudes is difficult because the vector nature of the magnetic field increases the complexity of anomalies from magnetic rocks. The most obvious approach to this problem is to reduce the data to the magnetic pole (RTP), where the presumably vertical magnetisation vector will simplify observed anomalies. However, RTP requires special treatment of north-south features in data observed in low magnetic latitudes due to high amplitude corrections of such features. Furthermore, RTP requires the assumption of induced magnetisation with the result that anomalies from remanently and anisotropically magnetised bodies can be severely disturbed.

The amplitude of the 3-D analytic signal of the total magnetic field produces maxima over magnetic contacts regardless of the direction of magnetisation. The absence of magnetisation direction in the shape of analytic signal anomalies is a particularly attractive characteristic for the interpretation of magnetic field data near the magnetic equator. Although the amplitude of the analytic signal is dependent on magnetisation strength and the direction of geological strike with respect to the magnetisation vector, this dependency is easier to deal with in the interpretation of analytic signal amplitude than in the original total field data or pole-reduced magnetic field. It is also straightforward to determine the depth to sources from the distance between inflection points of analytic signal anomalies.

Key words: analytic signal, magnetic interpretation, reduction to the pole, magnetic depth

Introduction

When dealing with 2-D magnetic field data, an important goal of data processing is to simplify the complex information provided in the original data. One such simplification is to derive a map on which the amplitude of the displayed function is directly and simply related to a physical property of the underlying rocks. For example, the gravity field over a body of a certain density contrast exhibits this simplicity. Baranov (1957) proposed converting 2-D magnetic data to 'pseudo-gravity' using a process that involves reduction to the pole (RTP) and vertical integration. Although Baronov's procedure is referred to as pseudo-gravity, the process does not imply that the distribution of magnetism in the Earth is necessarily related to the density distribution. It is intended only to simplify the interpretation of magnetic field data by thinking of magnetisation in the same way as density.

The essential ingredient in Baranov's (1957) pseudo-gravity process is the RTP since it presumably simplifies the vector nature of the magnetic field by making the field vertical. However, this process is not straightforward at low magnetic latitudes because of the very large amplitude corrections that must be applied to north-south trending features.

This paper proposes the use of 3-D analytic signal calculated from the total magnetic field (Nabighian, 1984; Roest *et al.*, 1992; MacLeod *et al.*, 1993) as a practical alternative to reduction to the pole from low magnetic latitudes. In fact, this technique has merit at all magnetic latitudes, but the benefits are most apparent near the magnetic equator.

Reduction to the Pole

The goal of reduction to the pole is to take an observed total magnetic field map and produce a magnetic map that would result had an area been surveyed at the magnetic pole. Assuming that all the observed magnetic fields of a study area are due to induced magnetic effects, pole reduction can be calculated in the frequency domain using the following operator (Grant and Dodds, 1972)

$$L(\Theta) = \frac{1}{[\sin(I) + i\cos(I)\cos(D-\Theta)]^2} \qquad (1)$$

where

- Θ is the wavenumber direction
- I is the magnetic inclination, and
- D is the magnetic declination.

From eq. (1), it can be seen that as I approaches 0 (the magnetic equator), and (D-Θ) approaches $\pi/2$ (a north-south feature), the operator approaches infinity. Figure 1 illustrates this effect by comparing the magnetic anomalies over an east-west and north-south vertically dipping dyke-like body. For the east-west striking dyke, the amplitude remains constant, but the shape changes. For the north-south striking dyke, the anomaly shape remains the same at all latitudes, but the amplitude is reduced as the inducing magnetic vector is rotated to be along strike at the magnetic equator, at which point the anomaly simply disappears.

The very large amplitude correction required for north-south features at low latitudes also amplifies the north-south components of noise and magnetic effects from bodies magnetised in directions different from the inducing field. Numerous authors have addressed the noise problem in the

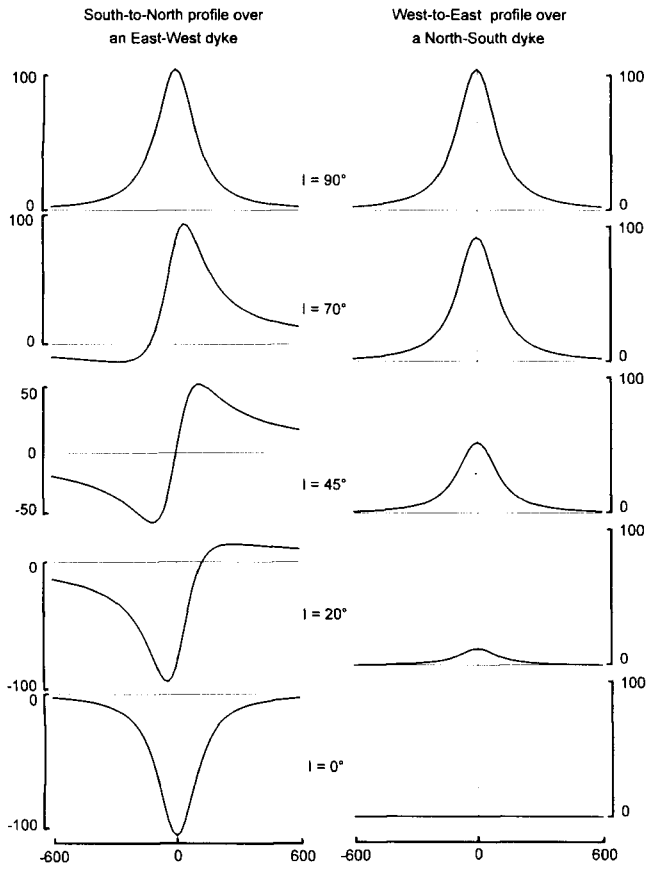

FIGURE 1
The shape of total magnetic field profiles over a vertically dipping dyke depends on the direction of the dyke. On the left, profiles are shown for an east-west striking dyke, and on the right profiles are shown for a north-south striking dyke. Reduction to the pole involves correcting the shape of east-west features and correcting the amplitude of north-south features to produce the same profile as would be observed at an inclination of 90°.

published literature. The methods either modify the amplitude correction in the magnetic north-south direction using frequency domain techniques (Hansen and Pawlowski, 1989; Mendonca and Silva, 1993), or calculate an equivalent source in the space domain (Silva, 1986). The simplest and most effective technique used in the MAGMAP FFT processing system developed by Grant and Dodds (1972) uses a second inclination (I') to control the amplitude of the filter near the equator.

$$L(\Theta)=\frac{1}{[\sin(I')+i\cos(I)\cos(D-\Theta)]^2} \qquad (2)$$

In practice, (I') is set to an inclination greater than the inclination of the magnetic field (or less than the true inclination in the Southern hemisphere). By using the true inclination in the $i\cos(I)$ term, anomaly *shapes* will be properly reduced to the pole, but by setting ($|I'| > |I|$), unreasonably large amplitude corrections are avoided. Controlling the RTP operator then becomes a matter of choosing the smallest I' that still gives acceptable results. This will depend on the quality of the data and the amount of non-induced magnetisation present in the area under study.

Figure 2 illustrates the application of the Grant and Dodds (1972) method of RTP processing on a simple model magnetised by induction and remanence. Note that when the body is magnetised only by induction (Fig. 2a), a reasonable RTP can be produced using eq. (1), the result of which is shown in Fig. 2c. However, adding remanence to the same body produces the total field anomaly shown in Fig. 2b, and the RTP process produces the very poor result shown in Fig. 2d. When remanent effects such as these are recognised, the amplitude inclination I' in eq. (2) can be increased to diminish the problem, as shown in Fig. 2f. However, this correction is at the expense of the RTP for the induced prism shown, which is shown in Fig. 2e. Adding noise to the data will introduce similar problems, although noise rejection filters can be designed to address the specific characteristics of the noise, which is often line-to-line levelling error.

Given these difficulties with RTP, and the original objective of simplifying the magnetic field, it would seem preferable to produce a result that simply provides a measure of the amount of magnetisation, regardless of direction.

3-D Analytic Signal

Nabighian (1972; 1974) developed the notion of 2-D analytic signal, or energy envelope, of magnetic anomalies. Roest *et al.* (1992) showed that the amplitude (absolute value) of the 3-D analytic signal at location (x,y) can be easily derived from the three orthogonal gradients of the total magnetic field using the expression

$$|A(x,y)|=\sqrt{\left(\frac{dT}{dx}\right)^2+\left(\frac{dT}{dy}\right)^2+\left(\frac{dT}{dz}\right)^2} \qquad (3)$$

where

$A(x,y)$ is the amplitude of the analytic signal at (x,y), and
T is the observed magnetic field at (x,y).

An important comment at this point is the ease with which the analytic signal can be calculated with commonly available computer software. The x and y derivatives can be calculated directly from a total magnetic field grid using a simple 3×3 filter, and the vertical gradient is routinely calculated using Fast Fourier Transform (FFT) techniques.

The analytic signal anomaly over a 2-D magnetic contact located at (x=0) and at depth h is described by the expression (after Nabighian, 1972)

$$|A(x)|=\alpha\frac{1}{(h^2+x^2)^{1/2}} \qquad (4)$$

where α is the amplitude factor

$$\alpha=2M\sin d(1-\cos^2(I)\sin^2(A)) \qquad (5)$$

and

h is the depth to the top of the contact,
M is the strength of the magnetisation,
d is the dip of the contact,
I is the inclination of the magnetisation vector, and
A is the direction of the magnetisation vector.

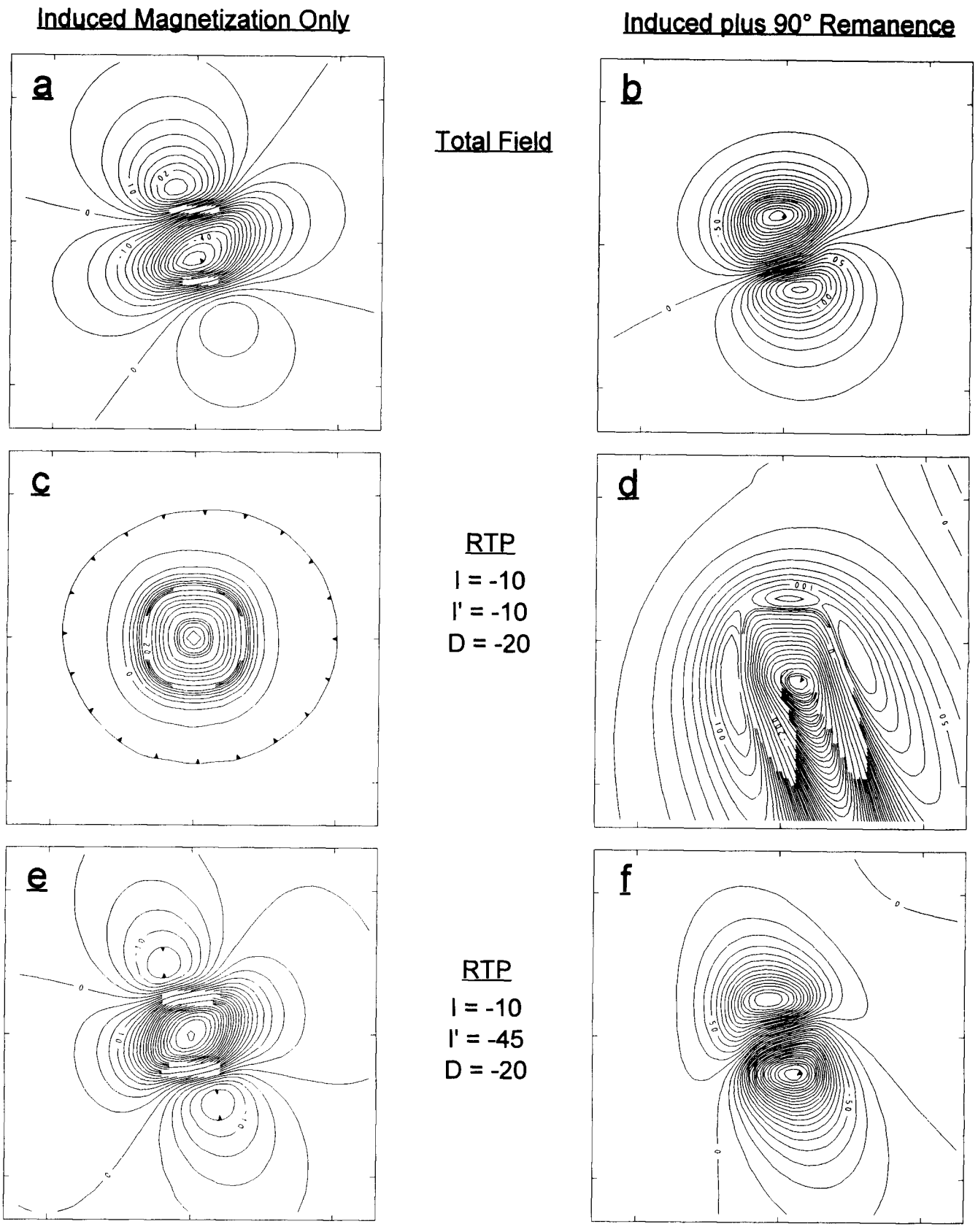

FIGURE 2
RTP applied to synthetic data for a depth limited prism 200×200 units square, 100 units thick, 50 units deep. (a) shows the magnetic field that results from induced magnetisation only in a field with an inclination of −10°, and declination 20° West, and (b) shows the same prism in the same inducing field, but with vertical remanence. (c) and (d) are the RTP results using equation (1) applied to (a) and (b) respectively. (c) shows the desired results but (d) shows a severely distorted anomaly after RTP. Applying equation (2) with an amplitude inclination (I') set to 45° produces the results shown in (e) and (f). A more acceptable anomaly is produced for the remanently magnetised prism (f), but at the expense of distortion in the induced prism (e).

The analytic signal described by eq. (4) is a simple bell-shaped function in which all directional terms are contained in the amplitude factor α, which is a constant. Therefore, only the amplitude of the analytic signal is affected by the vector components of the model. The shape of the analytic signal is dependent only on depth.

Similarly, it can be shown that the analytic signal anomaly over a 2-D magnetic sheet (or dyke) is described by the expression

$$|A(x)| = \alpha \frac{1}{(h^2+x^2)} \tag{6}$$

and over a cylinder

$$|A(x)| = \alpha \frac{2}{(h^2+x^2)^{\frac{3}{2}}} \tag{7}$$

Figure 3 shows the results of analytic signal processing over the same simple prism model used for reduction to the pole in Fig. 2. The use of a 3-D perspective presentation is to show how the amplitude of the analytic signal peaks over the edges of the model. Note that the amplitude of the peaks is proportional to the magnetisation at the edge as defined by eq. (5). In this case, the prism width is four times the depth. For widths less than the depth, the peaks of the analytic signal will merge.

MacLeod *et al.* (1993) showed how the analytic signal could be calculated from the vertical integral of the magnetic field in order to produce a result that was more similar to the analytic signal of pseudo-gravity. This had the effect of emphasising deeper, or more regional, information in the magnetic field and diminishing surface noise.

Depth from Analytic Signal

The analytic signal shape can be used to determine the depth to the magnetic sources. Atchuta Rao *et al.* (1981) and Roest *et al.* (1992) used the anomaly width at half the amplitude to derive the depths. Atchuta Rao *et al.* (1981) also used other characteristics of the analytic signal (which they referred to as 'complex gradient') to help resolve the effect of overlapping edges. The following relationships can be derived directly from eqs (4), (6) and (7).

For a contact

$$x_{\frac{1}{2}} = 2\sqrt{3}h = 3.46h \ ; \tag{8}$$

for a thin sheet (dyke)

$$x_{\frac{1}{2}} = 2h \ ; \text{ and} \tag{9}$$

for a horizontal cylinder

$$x_{\frac{1}{2}} = 2(\sqrt[3]{4}-1)^{\frac{1}{2}}h = 1.533h \ , \tag{10}$$

where

$x_{\frac{1}{2}}$ is the width of the anomaly at half the amplitude
h is the depth to the top of the contact.

However, the measured amplitude of an anomaly can be in error due to overlapping anomalies, and even where the amplitude can be well determined for a single source, the resulting depth will be significantly in error if the correct model is not used.

We have taken the approach of using the distance between the inflection points of the analytic signal anomaly to determine the depth. The inflection points occur higher up the flanks of the anomaly and therefore should be less susceptible to interference from neighbouring anomalies.

Taking the second derivative of eqs (4), (6) and (7) with respect to x produces the following results:

For a contact

$$\frac{d^2|A(x)|}{dx^2} = \alpha \frac{2x^2-h^2}{(h^2+x^2)^{\frac{5}{2}}} \tag{11}$$

$$x_i = \sqrt{2}h = 1.414h \ ; \tag{12}$$

for a thin sheet (dyke)

$$\frac{d^2|A(x)|}{dx^2} = \alpha \frac{2(3x^2-h^2)}{(h^2+x^2)^3} \tag{13}$$

$$x_i = \frac{2}{\sqrt{3}}h = 1.155h \ ; \text{ and} \tag{14}$$

for a horizontal cylinder

$$\frac{d^2|A(x)|}{dx^2} = \alpha \frac{6(4x^2-h^2)}{(h^2+x^2)^{\frac{7}{2}}} \tag{15}$$

$$x_i = h \tag{16}$$

where

A is the analytic signal calculated from eq. (3),
α is the amplitude factor from eq. (5),
h is the depth, and
x_i is the width of the anomaly between inflection points.

Model tests show that results for a vertical cylinder are very close to those predicted by eq. (16).

Table 1 summarises the two approaches for determining depth from analytic signal anomalies. Note that using the width at half the amplitude and assuming a contact model, the true depth for dyke/sill bodies will be 1.73 times the modelled depth, and the true depth for a cylindrical body will be 2.25 times the modelled depth. In contrast, using the distance between inflection points the true depth for a dyke/sill body will be 1.24 times the modelled depth, and the true depth of a cylindrical source will be 1.41 times the modelled depth.

TABLE 1
Analytic signal anomaly widths as a function of depth (h)

Source geometry	Distance between inflection points	Width at half the amplitude
contact	1.414h	3.46h
dyke/sill	1.155h	2h
cylinder	1h	1.533h

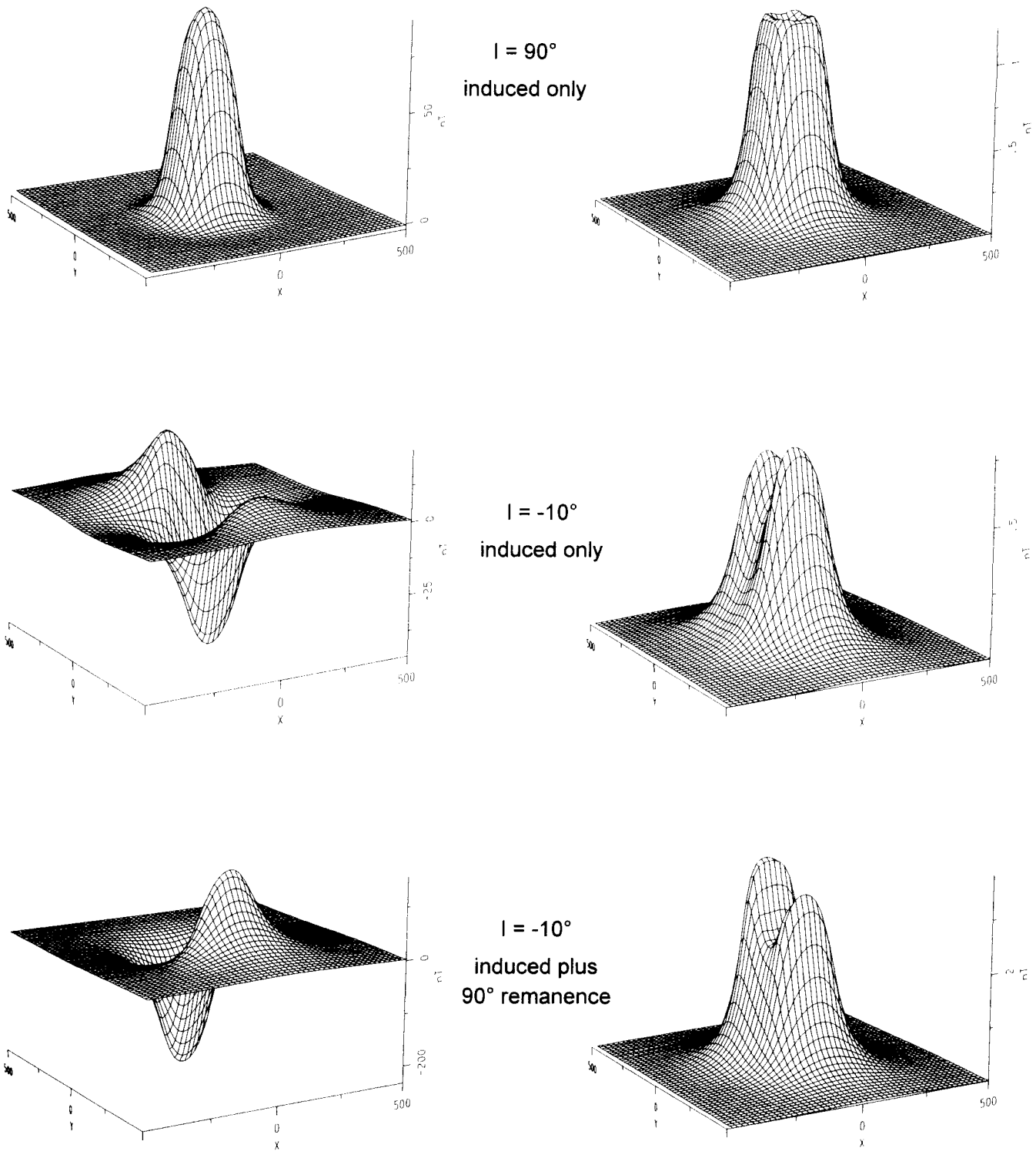

FIGURE 3
The analytic signal of the total magnetic field produces similar results regardless of the direction of magnetisation. In this case, the analytic signal is shown for the same model used in Fig. 2 under the same magnetic conditions. Note that the analytic signal peaks over the edges of the model, and the amplitude of the peak is proportional to the magnetisation at that edge.

Figure 4 shows the depth of a dyke-like source calculated from the inflection point widths as a function of the body width to depth ratio. These curves were compiled by measuring the width of the second horizontal derivative calculated from synthetic model curves. The second derivative was calculated by applying a simple three-point convolution filter (-0.5, 1, -0.5) to the synthetic curves. Note that when the body width is less than the depth, the apparent depth will increase with the width to a maximum of almost 2.5 times the true depth. When the width is greater than or equal to the depth, the method is able to distinguish the two edges of the body as separate edges. Results are shown for both an assumed dyke and sill, and the limiting cases agree with the theoretical prediction summarised in Table 1.

Figure 5 shows the effect of varying the thickness of a step as a function of depth. As the bottom of a step approaches the top, the model becomes more like a sill, and the sill model results approach the true depth. It is interesting to note when the thickness of a step is the same as the depth to the top, correct results are obtained using the step model, and as the thickness increases from that point, the apparent depth only increases to a maximum of 2% greater than the true depth, and then gradually returns to the depth predicted by theory as the thickness increases.

These results suggest that it is best to assume a contact model when working with more regional data. In the worst case, that of a very thin dyke or sill, the contact model will under-estimate the depth by 18%. Both the dyke and the sill model will over-estimate the depth of dyke-like bodies whose width approaches its depth. Vertical cylinder models can be rejected based on the fact that they produce a single isolated solution, and horizontal cylinders are rare.

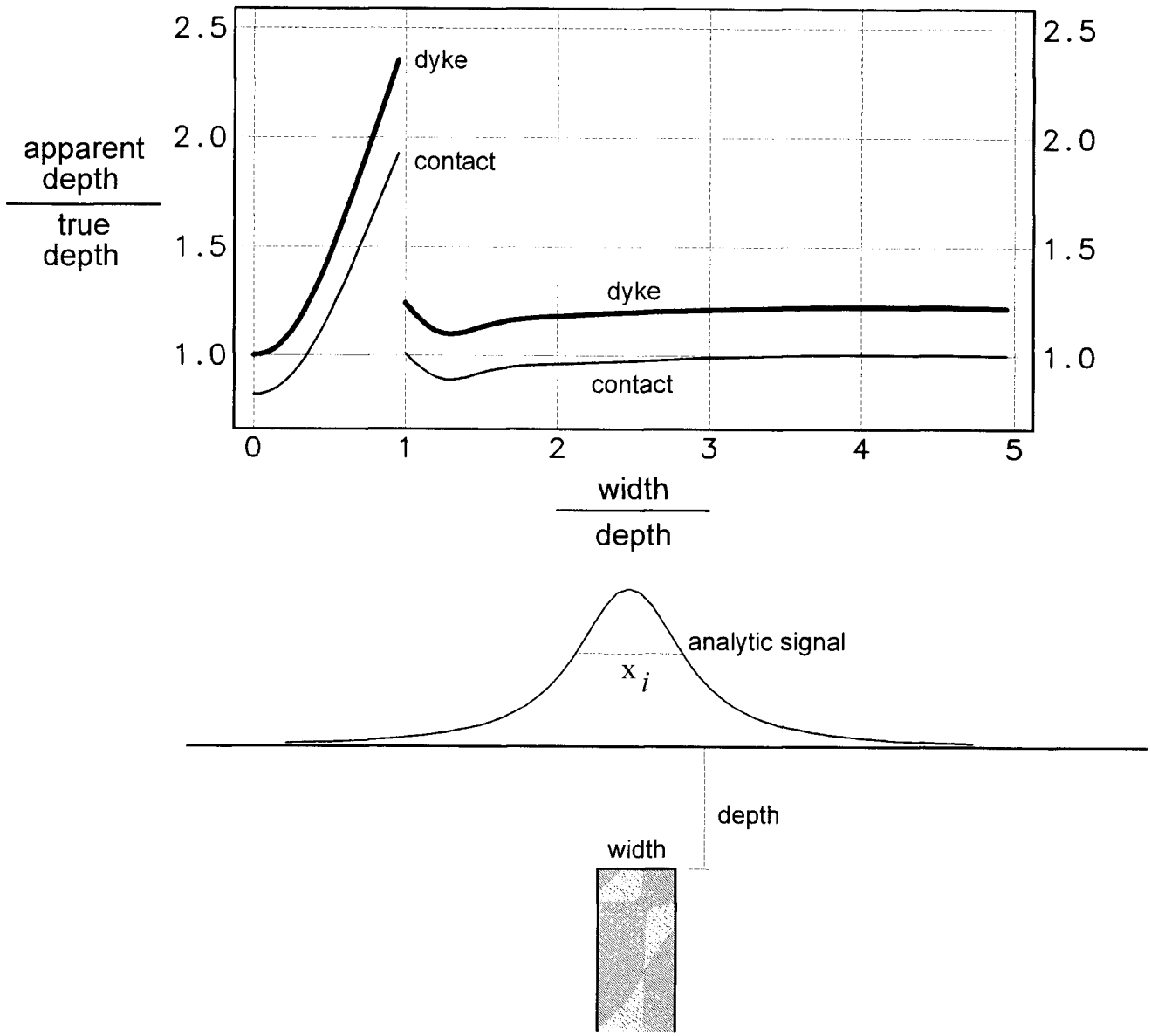

FIGURE 4
This figure shows the relationship between the apparent depth calculated from the width of the anomaly at the inflection points and the true depth as a function of the width for a dyke-like source. Results are shown assuming a dyke source (heavy line) and a contact source (light line). Note that where the width is less than the depth, the apparent depth increases to a maximum depth when the depth equals the width. Where the width is greater than the depth the anomaly is resolved into two edges, which produce separate depths as shown for width/depth values greater than 1.

Sangihe Island, Indonesia

An airborne magnetic and radiometric survey was conducted over the southern half of Sangihe Island, Indonesia, which forms part of a volcanic island arc extending over 400 km from the northeastern arm of Sulawesi to Mindanao in The Philippines. The helicopter survey was carried out on north-south lines with a nominal 200 m line separation, and a cesium total magnetic field sensor was towed at a nominal terrain clearance of 60 m.

The geology of Sangihe Island is characterised by Miocene to recently active calc-alkaline strata volcanoes, which become progressively younger northwards. Gold mineralisation occurs within a sequence of andesitic flows, sills and dykes, lithic and crystal tuffs and andesite porphyry intrusions. The main purpose of the survey was to help map areas of alteration within the volcanic pile. These are characterised by a reduced magnetic response, associated with the destruction of magnetite by mineralising fluids within the andesitic sequence. Areas of alteration are also characterised by potassium anomalies in the radiometric data. The magnetic data have been used to map lithology and major structural features which are important in focussing mineralisation. Because of a relatively young age of the rocks, remanent magnetisation was considered in the interpretation of the total magnetic field.

The original magnetic anomaly shown in Fig. 6 is asymmetric with a strong low on the north and a high on the south. Our interpretation of this feature is a roughly 1500 m long magnetic unit that strikes in an east-north-east direction. Strong remanent magnetisation is suspected because induced magnetised bodies at this latitude would produce an almost asymmetric low. In order to improve the interpretability of the data, standard RTP was performed using eq. (2), with the result shown in Fig. 7. It was necessary to use an amplitude inclination of 45° in order to reduce north-south

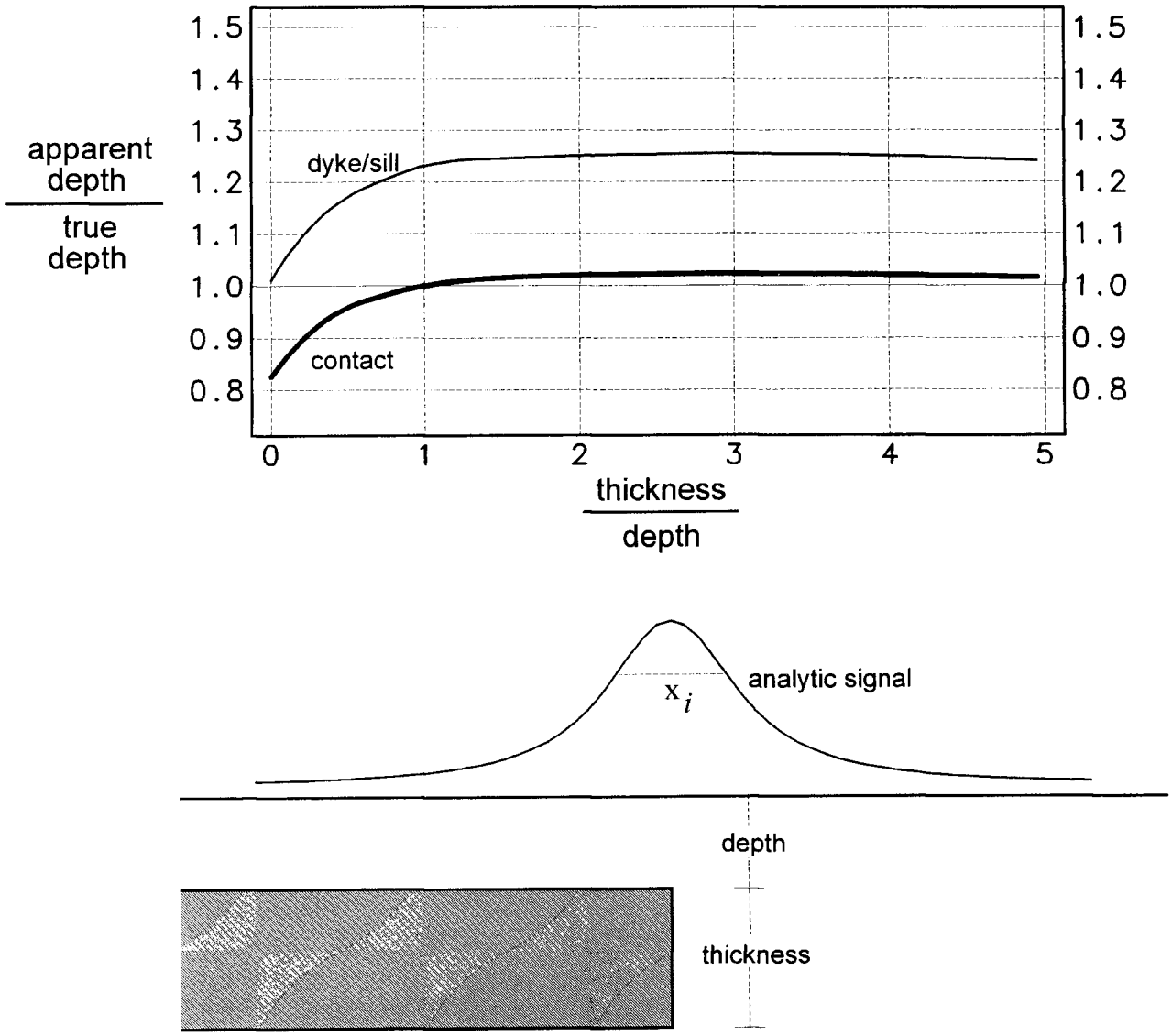

FIGURE 5
This figure shows the relationship between the apparent depth calculated from the width of the analytic signal anomaly between inflection points and the true depth as a function of the width for a step/contact source. Depths are calculated assuming a dyke source (light line) and a contact source (heavy line). Note that where thickness is equal to or greater than the depth, the contact model produces accurate results. As the thickness approaches 0, the step becomes a sill, and the dyke/sill model results are correct.

stretching of the anomaly, which further supports the suspicion of remanence. The pole-reduced anomaly could be interpreted as a shallow north-dipping body, which might explain the strong low, but this interpretation does not account for the undercorrected amplitude in the RTP.

Figure 8 shows the analytic signal calculated from the original total field data together with a simplified interpretation of the outline of the body and interpreted cross-cutting lineations/faults. Note how the analytic signal anomaly peaks clearly outline the north and south edges of the interpreted unit. Figure 9 shows the positive contours of the analytic signal after applying a sample 3×3 Laplacian filter, which has the following coefficients:

0	−0.25	0
−0.25	1	−0.25
0	−0.25	0

The Laplacian filter produces a curvature map in which inflection points in the original data are located at the zero contour. The contour map in Fig. 9 takes advantage of this by plotting only positive contours. The same effect can be achieved on a colour image by using a solid and contrasting colour for the negative parts of the Laplacian grid. From the Laplacian calculation, depths can be estimated by measuring the widths of the anomalies and applying the factors in Table 1. A number of measured depths are shown in Fig. 9 to

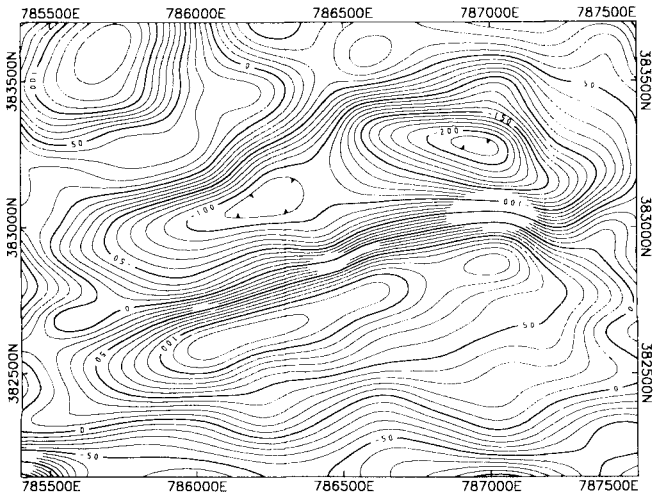

FIGURE 6
Total magnetic field contours over an apparently remanently magnetised body in Indonesia at a magnetic inclination of −10°. The source of the anomaly is interpreted to be roughly 1500 m in length and lies along the axis defined by the east-north-east trending anomaly.

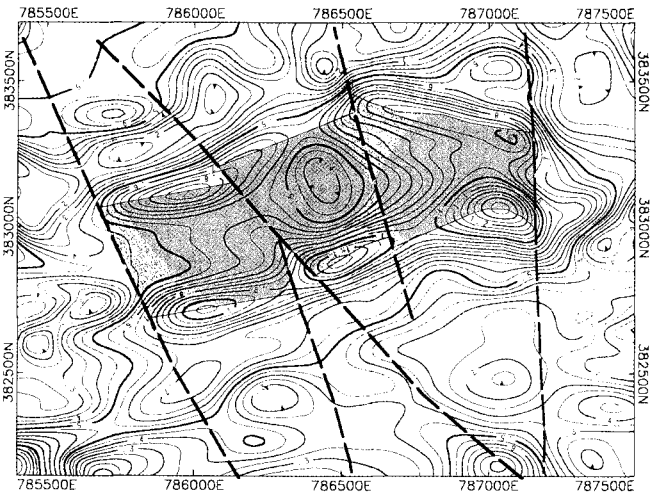

FIGURE 8
The analytic signal of the original total field data clearly shows anomalous highs which outline the body interpreted from Fig. 6. A simple interpretation of the outline of the body and the magnetic lineations/faults are shown for reference. The interpretation was based on the curvature plot shown in Fig. 9.

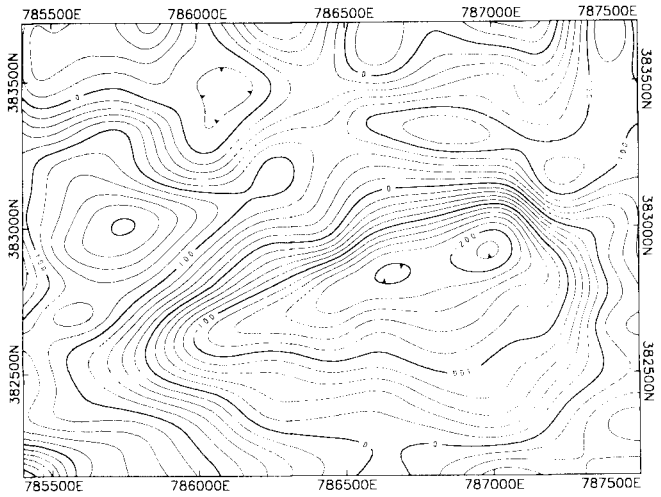

FIGURE 7
The anomaly shown in Fig. 6 has been reduced to the pole using eq. (2) with an amplitude inclination (*I'*) of 45°, which was necessary to reduce strong north-south stretching of the anomaly. The result is an asymmetric anomaly that might be interpreted as a shallow north-dipping body. However, this interpretation does not account for the north-south attenuation that was required. The fact that such attenuation was required confirms remanent magnetisation in the source.

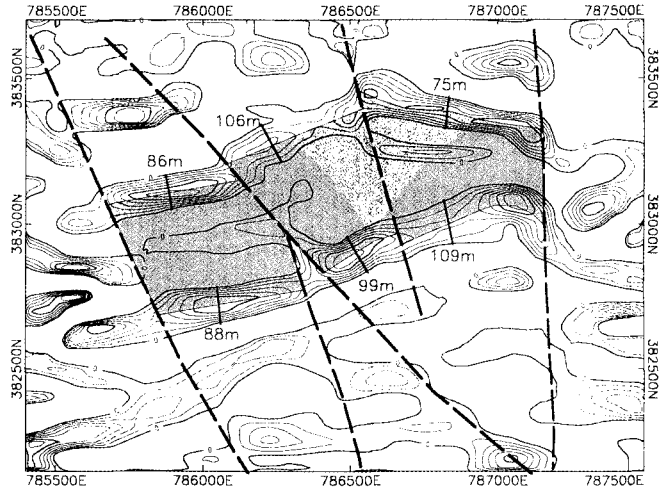

FIGURE 9
Applying a simple Laplacian filter to the analytic signal produces a curvature map from which inflection points are mapped by the zero contour. A simplified interpretation based on this data shows the outline of the source body and interpreted lineation/faults. Depths calculated from the curvature anomaly widths are also shown.

illustrate the measurement of anomaly widths. Automated methods similar to those described by Roest *et al.* (1992) can also be applied to produce depth maps.

Conclusions

Reduction to the pole attempts to simplify the magnetic field by rotating the magnetisation vector to be vertical. However, this technique presents significant problems when the direction of magnetisation is not in the same direction as the Earth's field, which is particularly important when the data have been collected at low magnetic latitudes. This problem can be partly overcome by modifying the amplitude correction of the pole reduction operator, but this must be done at the expense of distortion in anomalies from inductively magnetised rocks. In contrast, the analytic signal of the total magnetic field reduces magnetic data to anomalies whose maxima mark the edges of magnetised bodies, and whose shape can be used to determine the depths of those edges.

Since amplitude of analytic signal anomalies combines all vector components of the field into a simple constant, a good way to think of analytic signal is a map of magnetisation in the ground. With this in mind, stronger anomalies can be expected where the magnetisation vector intersects a magnetic contrast at an acute angle. As a result, inductively magnetised rocks at the equator will have stronger analytic signal at their north and south edges. The same thinking can be applied to remanently or anisotropically magnetised bodies which have magnetisation vectors in different directions.

Once an analytic signal grid is available, depths can be calculated by applying a Laplacian filter to the grid and measuring the distance between inflection points on anomalies of interest. This distance is directly proportional to the depth to the top of the contrast. Although a depth calculated in this way will depend on the assumed source model, it has been shown that the difference between source models will produce results generally accurate to within 20%. However, this method does not solve the common ambiguity between depth and thickness for dyke-like bodies where the width is less than or near the depth. Also, because an analytic signal anomaly simply marks a magnetic contrast, one does not know the sense of the contrast from the analytic signal alone. Because of this, the original total field map should be used to help resolve these aspects of an interpretation.

Acknowledgements

The authors would like to thank Aurora Gold Limited for providing the geophysical data from Sangihe Island and Geosoft Inc. for their support of this work. Thanks are also due to Sergio Vierra of WMC Brazil for proving the practical application of these techniques in his own work near the magnetic equator in South America.

References

Atchuta Rao, D., Ram Babu, H.V. and Sanker Narayan, P.V. (1981), 'Interpretation of magnetic anomalies due to dykes: The complex gradient method', *Geophysics* **46**, 1572–1578.

Baranov, V. (1957), 'A new method for interpretation of aeromagnetic maps: Pseudo-gravimetric anomalies', *Geophysics* **22**, 359–383.

Grant, F.S. and Dodds, J. (1972), 'MAGMAP FFT processing system development notes', Paterson Grant and Watson Limited.

Hansen, R.O. and Pawlowski, R.S. (1989), 'Reduction to the pole at low latitudes by Wiener filtering', *Geophysics* **54**, 1607–1613.

MacLeod, I.N., Vierra, S. and Chaves, A.C. (1993), 'Analytic signal and reduction-to-the-pole in the interpretation of total magnetic field data at low magnetic latitudes'. Proceedings of the third international congress of the Brazilian Society of Geophysicists.

Mendonca, C.A. and Silva, J.B.C. (1993), 'A stable truncated series approximation of the reduction-to-the-pole operator', *Geophysics* **58**, 1084–1090.

Nabighian, M.N. (1972), 'The analytic signal of two-dimensional magnetic bodies with polygonal cross-section: Its properties and use for automated anomaly interpretation', *Geophysics* **37**, 507–517.

Nabighian, M.N. (1974), 'Additional comments on the analytic signal of two-dimensional magnetic bodies with polygonal cross-section', *Geophysics* **39**, 85–92.

Nabighian, M.N. (1984), 'Toward a three-dimensional automatic interpretation of potential field data via generalised Hilbert transforms: Fundamental relations', *Geophysics* **49**, 780–786.

Roest, W.R., Verhoef, J. and Pilkington, M. (1992), 'Magnetic interpretation using the 3-D analytic signal', *Geophysics* **57**, 116–125.

Silva, J.B.C. (1986), 'Reduction to the pole as an inverse problem and its application to low-latitude anomalies', *Geophysics* **51**, 369–382.

This article has been cited by:

1. Lianghui Guo, Xiaohong Meng, Yaning Liu, Lei ShiA new wavenumber-domain method for magnetic reduction to the pole at low latitudes 1195-1199. [Abstract] [References] [PDF] [PDF w/Links]
2. Vinicius Hector Abud Louro, Vanessa Biondo Ribeiro, Marta Silvia Maria MantovaniGeophysical Exploration of the Buraco da Velha Deposit (RO, Brazil) 696-701. [Abstract] [References] [PDF]
3. Guoqing Ma, Lili Li, Danian HuangAlternative Analytic Signal Methods for the Interpretation of 2D Magnetic Anomaly Data 467-471. [Abstract] [References] [PDF]
4. V. Ramesh Babu, Subhash Ram, N. Sundararajan. 2007. Modeling and inversion of magnetic and VLF-EM data with an application to basement fractures: A case study from Raigarh, India. *GEOPHYSICS* **72**:5, B133-B140. [Abstract] [Full Text] [PDF]
5. Jeffrey D. Phillips, R. O. Hansen, Richard J. Blakely. 2007. The use of curvature in potential-field interpretation*. *Exploration Geophysics* **38**:2, 111-119. [Abstract] [Full Text] [PDF] [PDF w/Links]
6. Xiong LiMagnetic reduction to the pole at low latitudes: Practical considerations 718-722. [Abstract] [References] [PDF] [PDF w/Links]
7. Xiong Li. 2006. Understanding 3D analytic signal amplitude. *GEOPHYSICS* **71**:2, L13-L16. [Citation] [Full Text] [PDF]
8. Mark Pilkington, Pierre Keating. 2006. The relationship between local wavenumber and analytic signal in magnetic interpretation. *GEOPHYSICS* **71**:1, L1-L3. [Citation] [Full Text] [PDF]
9. Ahmed Salem, Dhananjay Ravat, Martin F. Mushayandebvu, Keisuke Ushijima. 2004. Linearized least-squares method for interpretation of potential-field data from sources of simple geometry. *GEOPHYSICS* **69**:3, 783-788. [Abstract] [References] [PDF]
10. George K. AsiamahThe South Ashanti Greenstone belt GEOTEM and magnetic survey- application to mineral exploration 1143-1146. [Abstract] [References] [PDF] [PDF w/Links]
11. Shanti Rajagopalan. 2003. Analytic signal vs. reduction to pole: solutions for low magnetic latitudes. *Exploration Geophysics* **34**:4, 257-262. [Abstract] [PDF] [PDF w/Links]
12. Ahmed Salem, Dhananjay Ravat. 2003. A combined analytic signal and Euler method (AN-EUL) for automatic interpretation of magnetic data. *GEOPHYSICS* **68**:6, 1952-1961. [Abstract] [References] [PDF]
13. Ahmed Salem, Dhananjay Ravat, Martin Mushayandebvu, Keisuke UshijimaEstimation of depth and shape factor from potential-field data over sources of simple geometry 724-726. [Citation] [PDF] [PDF w/Links]
14. John Paine, Mike Haederle, Marcus Flis. 2001. Using transformed TMI data to invert for remanently magnetised bodies. *Exploration Geophysics* **32**:3/4, 238-242. [Abstract] [PDF] [PDF w/Links]
15. Christopher J. Swain1. 2000. Reduction-to-the-pole of regional magnetic data with variable field direction, and its stabilisation at low inclinations. *Exploration Geophysics* **31**:1/2, 78-83. [Abstract] [PDF] [PDF w/Links]
16. Shu-Kun Hsu, Dorothée Coppens, Chuen-Tien Shyu. 1998. Depth to magnetic source using the generalized analytic signal. *GEOPHYSICS* **63**:6, 1947-1957. [Abstract] [References] [PDF]
17. Shanti Rajagopalan, David Clark, Phillip Schmidt. 1995. Magnetic mineralogy of the Black Hill Norite and its aeromagnetic and palaeomagnetic implications. *Exploration Geophysics* **26**:2/3, 215-220. [Abstract] [PDF] [PDF w/Links]
18. P.J. Gunn, D. Maidment, P. Milligan. 1995. Interpreting aeromagnetic data in areas of limited outcrop: an example from the Arunta Block, Northern Territory. *Exploration Geophysics* **26**:2/3, 227-232. [Abstract] [PDF] [PDF w/Links]